DNA AND CELL BIOLOGY
Volume 33, Number 5, 2014

Pp. 301–310
DOI: 10.1089/dna.2013.2229

Ultrasound Microbubble-Mediated Delivery of Integrin-Linked Kinase Gene Improves Endothelial Progenitor Cells Dysfunction in Pre-Eclampsia

Kai Cui,[1] Ting Yan,[1] Qingqing Luo,[1] Yanfang Zheng,[1] Xiaoxia Liu,[1] Xiaoyu Huang,[2] and Li Zou[1]

Pre-eclampsia (PE) is a specific vascular complication in pregnancy whose precise mechanism is still unclear. We hypothesized that endothelial progenitor cells (EPCs), the precursor of endothelial cells, might be impaired in patients with PE and hold a great promise for the treatment of PE. In the present study, we analyzed the EPCs number and expression of integrin-linked kinase (*ILK*) in PE patients. We confirmed that both EPCs number and *ILK* expression were diminished in PE patients. Next, we transfected EPCs with *ILK* gene using ultrasonic microbubble technique (UMT) for the first time, as UMT is a novel type of gene transfer technology showing promising applications in stem cells apart from EPCs. To further investigate the transfection efficiency of UMT, RT-PCR analysis and western blot were used to examine the messenger RNA (mRNA) and protein level of ILK. After transfection of the *ILK* gene, EPCs function was tested to illustrate the role of ILK in cell proliferation, apoptosis, migration, and secretion. The results of the *in vitro* study suggested that UMT, a novel gene delivery system, could be considered a potent physical method for EPCs transfection. Moreover, the growth and angiogenetic properties of EPCs are enhanced by introducing ILK. This study may afford a new trend for EPCs transfection and gene therapy in PE.

Introduction

Pre-eclampsia (PE) is a life-threatening hypertensive disease of pregnancy that develops after 20 weeks of gestation. The condition is characterized by the presence of endothelial dysfunction and vasospasm that result in hypertension and placental ischemia. Research conducted in recent years has shown that endothelial progenitor cells (EPCs), a heterogeneous group of endothelial cell precursors, have a potential role in maintaining vascular integrity (Asahara, 1997). EPCs possess the capacity to migrate to ischemic sites, differentiate into endothelial cells, and release a source of paracrine factors for angiogenesis (Hill *et al.*, 2003). Our group has confirmed that PE reduces EPCs number and impairs EPCs function as evident in our previous research (Yan *et al.*, 2013). Studies also have demonstrated that small for gestational age infants were associated with lower maternal EPC number and reduced migratory function (King *et al.*, 2013). The existing evidence suggests that aberrant vessel formation may be contributed by the impaired availability or function of the EPCs forming them (Lin *et al.*, 2009). Therefore, EPCs could be both diagnostic tools and direct targets of medical interventions for PE. At present, EPCs *ex vivo* therapy has been expected to be a novel treatment conducted in ischemic and cardiovascular diseases (Hill *et al.*, 2003). Although there are extensive studies of EPCs transplantation outside of pregnancy, its use in the therapy of PE is rare with regard to effectiveness and safety concerns.

Due to limited endogenous pool and the possible functional impairment of EPCs associated with PE, we should first modify EPCs *in vitro* by introducing a therapeutic gene into EPCs to overcome such limitations (Churdchomjan *et al.*, 2010). In this research, we focused on integrin-linked kinase (*ILK*) gene, a ubiquitously expressed scaffold protein that functions as an important regulator of cell–ECM interaction (Hannigan *et al.*, 1996; Wu and Dedhar, 2001). ILK is involved in central cell biological processes such as cell adhesion, proliferation, migration, survival, and differentiation (Wang *et al.*, 2011). Moreover, ILK has a certain therapeutic effect in ischemia vascular diseases such as myocardial infarction (Cho *et al.*, 2005; Song *et al.*, 2009), attributing to its pivotal role in blood vessel formation during embryogenesis and other physiological settings (Malan *et al.*, 2013). These findings suggest that both EPCs and ILK play a vital role in angiogenesis. Therefore,

Departments of [1]Obstetrics and Gynecology and [2]Ultrasound, Union Hospital, Huazhong University of Science and Technology, Wuhan, China.

promotion of the angiogenic property of EPCs could be realized by transferring *ILK* genes into EPCs *in vitro*, so as to realize stem cell therapy in the treatment of PE.

A successful gene modification of EPCs mainly relies on the development of the gene delivery vector. Currently, there are a variety of gene delivery methods, which are mainly divided into viral and non-viral vector systems (Patil *et al.*, 2005). The use of viral vectors is considered as exhibiting high transfection efficiency yet poor safety and organ specificity (Vannucci *et al.*, 2013). Thus, the development of high-performance and non-viral gene delivery vehicles is promising and may have a better chance to circumvent some of the problems possibly occurring with viral vectors. To eliminate the concern about the safety of EPCs transfection, we employed the ultrasonic microbubble technique (UMT), a novel type of non-viral gene transfer technology that has achieved great breakthroughs. UMT ensures that gene transfection is both efficient and targeted (Chen *et al.*, 2006; Suzuki *et al.*, 2011). It not only realizes the location ''blasting'' of microbubbles (Bekeredjian *et al.*, 2007), but also transiently perforates the cell membrane, which enables the delivery of plasmid DNA (pDNA) or drugs into the cell (Cavalli *et al.*, 2012). The intake of genes or drugs into cells is significantly increased so that the effect of treatment is markedly improved (Xing *et al.*, 2008).

PE has been the focus of medical researchers over the years. However, the role of EPCs in the pathogenesis and therapy of PE is as yet unknown. In this research, we showed that ILK represents a common signal pathway linking EPCs deficiency and endothelial dysfunctional states, with PE. Besides, we transfected EPCs with *ILK* pDNA using the ultrasonic microbubble for the first time. Results showed that ultrasonic microbubble gene delivery is a safe, effective, and easy-to-apply method. UMT-mediated up-regulation of *ILK* pDNA expression would improve the angiogenic properties of EPCs. Our study will provide a better understanding of *ILK* and its role in EPCs function, and *ILK* gene-modified EPCs could pose as a potential treatment of PE.

Materials and Methods

Study population

The study was conducted at the Department of Obstetrics and Gynecology, Union Hospital, Huazhong University of Science and Technology (HUST), from December 2012 to May 2013. Blood samples for EPCs culture were obtained in a case-control design from 12 women with PE and from 9 women with an uncomplicated pregnancy (control). All subjects were in the third trimester of pregnancy. PE was defined as hypertension (blood pressure higher or equal to 140/90 mmHg on two occasions separated by 6°h) and proteinuria (300 mg/24°h) that occurred after 20 weeks of gestation, in women with previously normal blood pressure. Controls were healthy subjects without pregnancy complications or chronic medical problems (Chesley, 1980). All the subjects underwent cesarean section (controls undergoing cesarean section due to their own demands). Table 1 lists clinical characteristics of the two groups. Written informed consent was obtained from the women who agreed to participate in the study, which was approved by the ethics committee of Tongji Medical College.

Table 1. Characteristics of Study Subjects

	Pre-eclampsia (n = *12*)	*Normal* (n = *9*)	p-*Value*
Maternal age (years)	31.2 ± 4.0	29.3 ± 3.1	> 0.05
BMI	27.1 ± 3.2	26.8 ± 4.4	> 0.05
Gestational weeks at delivery	34.3 ± 2.8	37.9 ± 1.7	< 0.05
SBP at delivery	158.1 ± 9.7	121 ± 12.6	< 0.05
DBP at delivery	100.2 ± 11.7	78.9 ± 8.4	< 0.05
Proteinuria	100% (12/12)	0% (0/9)	< 0.05
S/D ratio of umbilical artery	3.1 ± 0.9	2.4 ± 0.6	< 0.05
Birthweight (g)	2228 ± 516	2612 ± 619	< 0.05

Data are listed as mean ± SD or percentage (number/total). Proteinuria is defined in the ''Materials and Methods'' section.

BMI, body mass index in pregnancy (kg/m^2); DBP, diastolic blood pressure; SBP, systolic blood pressure; S/D ratio, systole/diastole (S/D) ratio.

Cell culture and EPCs characterization

Previous studies have demonstrated that EPCs can be differentiated from mononuclear cells (MNCs) in peripheral blood (Hur *et al.*, 2007). MNCs was isolated from 30 mL peripheral blood as previously described (Asahara, 1997). Briefly, MNCs were fractionated from other components of peripheral blood by Ficoll density gradient centrifugation (400 *g*, 30 min, 20°C) according to the manufacturer's instructions. After purification with phosphate-buffer solution (PBS), MNCs were resuspended at a final concentration of 1×10^6 cells/mL in endothelial basal medium-2 (EBM-2; Lonza) that was supplemented with EGM-2-MV-SingleQuots (Lonza), and seeded on fibronectin-coated (Sigma-Aldrich) six-well culture dishes (Corning). After 3 days of culture, non-adherent cells were discarded, and the medium was replaced every 2 days. All experiments were performed with EPCs at day 7. To identify the ability of cells to incorporate DiI-acetylated-low-density lipoprotein (DiI-Ac-LDL) and FITC-labeled Ulex europaeus agglutinin-I (FITC-UEA-I), attached cells were incubated with DiI-Ac-LDL (2.4 mg/mL; Molecular Probes) in complete EGM-2 media at 37°C for 4 h. Cells were washed thrice with PBS and fixed with 2% paraformaldehyde, then incubated with FITC-UEA-I (10 mg/mL; Sigma-Aldrich) for 1 h. Dual-staining cells for both DiI-Ac-LDL and FITC-UEA-I were identified as differentiating EPCs with a laser scanning confocal microscope (Leica). Dual-staining cells in control and PE groups were counted by two independent experimenters. To compare the basal expression of *ILK* in EPCs from controls and PE patients, endogenous *ILK* expression in the cells was quantified by immunoblot and RT-PCR analysis.

Preparation of pIRES-ILK-Dsred plasmid and microbubbles

This study used two pDNA vectors. The empty plasmid containing red fluorescent protein (Dsred) was used to determine the percentage of transfection efficiency and acted as a negative control. The pIRES-ILK-Dsred plasmid was constructed by inserting the *ILK* complementary DNA (cDNA) into the plasmid and used for functional gene

transfection. The constructed plasmid was sequenced by BGI (a genomic research company; web link: www.genomics.cn/en/index). To prepare the lipid microbubble, we mixed SonoVue (Bracco) with 5 mL of a 0.9% saline solution immediately before use. SonoVue microbubble contains sulfur hexafluoride gas and has a phospholipid monolayer shell. The concentration of the microbubbles was added to each well at a 10% concentration, with a mean diameter of 2.5 μm.

Ultrasound parameters and transfection

To determine the optimal ultrasound parameters for transfection, ultrasound exposures were administered in EPCs at various intensities (0.25, 0.5, 0.75, and 1.0 W/cm^2) and at various time points (30 and 60 s). Next, the cell viability was detected. In the experiments, the ultrasound parameters for EPCs transfection were as follows: continuous wave, 300 kHz, 0.5 W/cm^2, 30 s, and a 10% concentration of microbubbles (Chen *et al.*, 2012; Han *et al.*, 2012). On 7 days of culture, EPCs from PE patients were seeded in each well of 24-well culture plates with 5×10^5 cell density and cultured in complete DMEM medium for 24 h before transfection. Next, the cells were divided into three groups as follows: (i) control, without transfection; (ii) UMT + empty plasmid, treated with ultrasonic microbubble technique (UMT) and empty plasmid only; and (iii) UMT + ILK, treated with UMT and pIRES-ILK-Dsred plasmid. After 48 h of incubation, DNA transfection efficiency was determined by observing the expression of red fluorescent protein (Dsred) using a fluorescence microscope. Final transfection efficiency in each transfection well was represented by the percentage of cells expressing fluorescent protein.

Trypan blue staining

When the cells reached 90% confluence, they were exposed to different intensities of ultrasound (0.25, 0.5, 0.75, and 1.0 W/cm^2) and different radiation times (30 and 60 s) respectively. After incubation for 24 h, the cells were washed, trypsinized, and resuspended with PBS. After that, the cells were treated with an equal volume of 0.2% trypan blue and incubated at room temperature for 4 min. Next, the cells were loaded into a hemocytometer. Survival cells excluding trypan blue were counted in three separate fields under a microscope. Survival rate = (number of survival cells/number of total cells) × 100%.

Detection of ILK *messenger RNA and protein expression*

The cells were harvested and subjected to qRT-PCR to determine the messenger RNA (mRNA) expression of ILK. Total RNA was extracted from EPCs using TRIZOL reagent (Invitrogen) and reverse transcripted into cDNA with a random primer and a reverse transcriptase (Takara). The resultant cDNA was amplified using a specific primer pair for ILK: 5′-TTC AAA CAG CTT AAC TTC CT-3′, reverse primer: 5′-ACT CGA CAT GTC TGC TGA GC-3′. Primer sequences for GAPDH, forward primer: 5′-ACCAC AGTCCATGCCATCAC-3′, reverse primer: 5′-TCCACCA CCCTGTTG CTGTA-3′. GAPDH were used as internal controls. Each reaction was performed in triplicate by employing SYBR Premix Ex Taq™ (Takara) on a Real-time PCR system (Applied Biosystems). The cycling program consisted of 40 cycles, and it was performed as follows: 95°C for 15 s, 62°C for 15 s, and 72°C for 45 s after an initial denaturation step (95°C for 2 min). The results were subjected to melting curve analysis. The relative gene expression of ILK was analyzed using $2^{-\Delta\Delta Ct}$ method.

Western blotting analysis

EPCs were washed in ice-cold PBS and lysed by cold RIPA buffer (200 μL/well; Beyotime). Lysates were centrifuged at 12,000 rpm for 30 min, and protein concentration was determined with BCA protein assay kit (Beyotime). The supernatant containing proteins were stored at −20°C. Proteins were separated by 10% sodium dodecyl sulfate–polyacrylamide electrophoresis gel. After electrophoresis, the proteins were transferred to a nitrocellulose membrane by electroblotting and blocked in 5% non-fat milk in 1× Tris-buffered saline with 0.1% Tween-20 (TBST). The blots were incubated overnight with the primary antibody (1:2000) at 4°C and washed thrice with TBST. After washing, the blots were incubated with the secondary antibody (1:2000) at room temperature for 1 h, and ECL-PLUS (Amersham Biosciences) was used for detection. β-Actin served as an internal control to assess protein loading. All the antibodies used in this study (ILK, vascular endothelial growth factor [VEGF], β-actin, and horseradish peroxidase-conjugated secondary antibodies) were purchased from Cell Signaling Technology.

Cell viability and apoptosis

Cell viability was detected by MTT assay. The transfected EPCs were harvested using 0.25% Trypsin–EDTA and washed twice using PBS. Next, the cells were seeded into 96-well culture plates with 1.0×10^3 cells/well. Twenty microliter of MTT (5 mg/mL; Sigma-Aldrich) reagent was added to each well and incubated at 37°C for 4 h. The medium was removed, and dimethyl sulfoxide (DMSO) was added to each well before the absorbance was measured at 490 nm using a microplate reader (Model 550; Bio-Rad). Cell apoptosis was evaluated by the annexin V-FITC apoptosis detection kit (Calbiochem). All cells (floating and attached) were harvested and stained for apoptotic and necrotic markers. Flow cytometry analyses were carried out with FACS Aria II and DiVa software. Percent apoptosis is the number or apoptotic cells divided by the number of all analyzed cells. A TUNEL assay for the detection of apoptotic cells was also conducted (DeadEnd™ Colorimetric TUNEL System; Promega Corp.) as previously described (Gao *et al.*, 2013). Finally, TUNEL-positive cells per field were counted in three random fields, and the counts were averaged.

Immunocytochemistry

Cells cultured on coverslips (Thermanox from NUNC) in EBM-2 medium were rinsed twice in PBS. For the detection of Ki67, samples were incubated in 4% formaldehyde for 15 min, followed by incubation in 96% ethanol for 10 min. Samples were then rinsed in water before heat-induced epitope retrieval for 15 min in Tris-EGTA buffer,

pH 9.0 at 95°C. Mouse-anti-Ki67 (1:100; Invitrogen, Life Technologies) were used as primary antibodies, followed by incubation with the appropriate secondary antibody (Dako), labeled streptavidin-horseradish-peroxidase (Dako), DAB chromogen, and 0.2% osmium tetroxide (Sigma Chemicals). Positive cells were quantified and expressed as percentages.

Cell migration assay

EPC migration was evaluated using transwells (8-μm pore size; Corning). Twenty-four hours after transfection, EPCs were trypsinized and resuspended in medium containing 1% fetal bovine serum (FBS). About 5×10^4 cells were placed in the upper chamber, and the lower chamber was filled with 500 μL of medium containing 10% FBS and 50 ng/mL VEGF as a chemoattractant. After incubation at 37°C for 24 h, non-migrated cells on the upper side of the membrane were removed. The cells on the lower side of the filter were washed with PBS and fixed with 2% paraformaldeyde. The cells were stained with crystal violet. Next, the cells in three randomly selected 100× magnification fields per transwell were counted manually by two independent observers. Each experiment was performed in triplicate.

Enzyme-linked immunosorbent assay

Enzyme-linked immunosorbent assay (ELISA) was executed to measure the concentrations of VEGF in the medium post-transfection. Forty-eight hours after transfection, the culture supernatants of transfected EPCs of different groups were collected and stored at −80°C after centrifugation. The amount of VEGF in each supernatant was quantified by a human VEGF immunoassay kit (R&D Systems) according to the recommended procedures. The optical density was measured by a microplate reader (Model 550; Bio-Rad) at dual wavelengths of 450–540 nm.

Statistical analysis

All values were expressed as mean ± standard deviation. Statistical analyses were performed using the SPSS 13.0 package. Comparisons between groups were performed by the Student's *t*-test and one-way analysis of variance (ANOVA) test. A *p*-value of < 0.05 was considered statistically significant. All data were obtained from three independent experiments.

Results

Clinical characteristics of the study population

The clinical characteristics of the total group are summarized in Table 1. Women in the PE group showed a significantly higher systolic and diastolic arterial pressure (158.1 ± 9.7 vs. 121 ± 12.6 mmHg and 100.2 ± 11.7 vs. 78.9 ± 8.4 mmHg, respectively, $p < 0.05$) than controls, as well as an S/D ratio of the umbilical artery (3.1 ± 0.9 vs. 2.4 ± 0.6, $p < 0.05$). Gestational age at delivery was also significantly different between controls and PE patients. No significant differences were observed in maternal age. These differences revealed vasospasm and inadequate blood supply of the fetus.

Characterization of EPCs

We followed the culture of MNCs in endothelial cell growth medium for at least 1 week. MNCs gradually become spindle-shaped cells with a low nuclear/cytoplasmic ratio at 1 week after seeding (Fig. 1A–C). EPCs displayed a comprehensive phenotype of uptaking DiI-Ac-LDL uptake and UEA-I lectin binding as shown in Figure 1D.

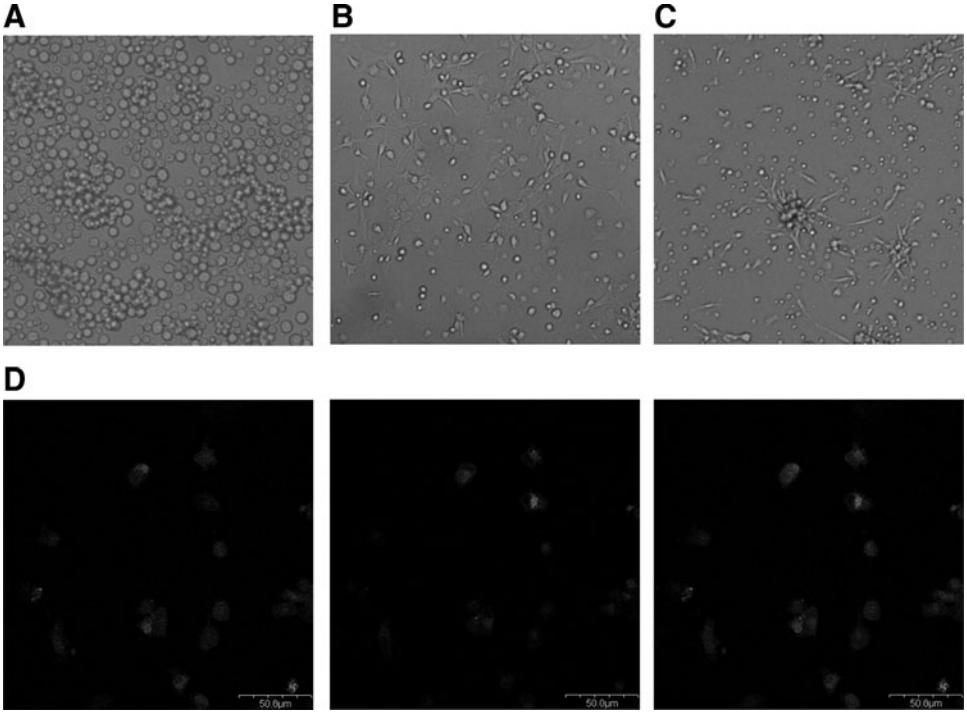

FIG. 1. Characteristics of isolated endothelial progenitor cells (EPCs) from cord blood. **(A)** Cord blood mononuclear cells immediately after plating **(B)** attached cells at 3 days after seeding. **(C)** A week after seeding, they were elongated and had a spindle shape. **(D)** At 7 days of culture, the representative pictures of dual-stained EPCs in confocal microscopy. Middle pannel represents fluorescent staining of DiI-acetylated-low-density lipoprotein (DiI-Ac-LDL), and left panel represents fluorescent staining of FITC-conjugated Ulex europaeus agglutinin-I (UEA-I).

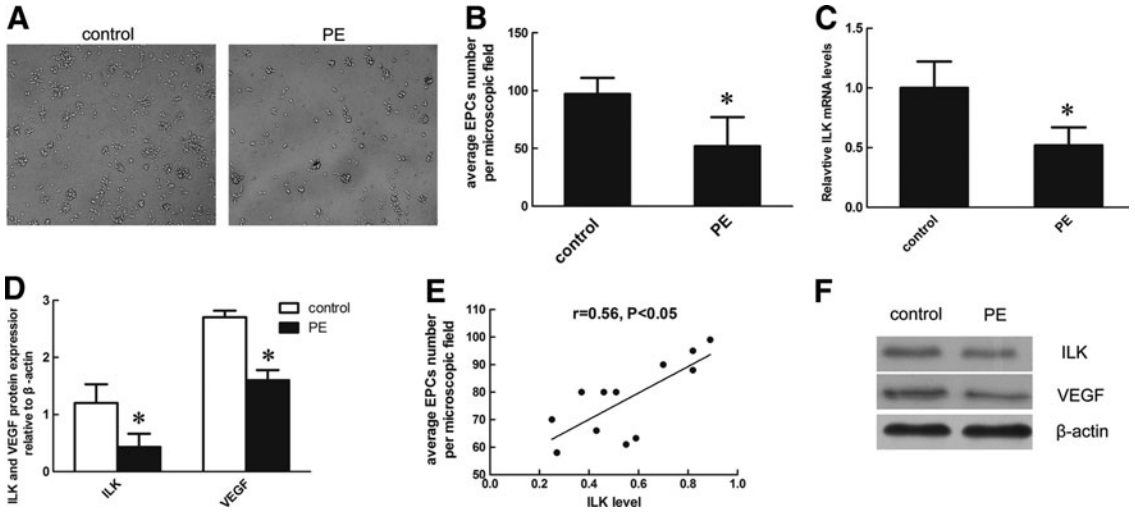

FIG. 2. EPCs number and basal expression of integrin-linked kinase (*ILK*) in two groups. **(A)** Representative microscopic images of EPCs from healthy control and pre-eclampsia (PE) patient after 7 days of culture. **(B)** Statistical analysis of EPCs numbers in PE group and control group. **(C)** Densitometry of *ILK* messenger RNA (mRNA) relative to GAPDH was determined using semi-quantitative analysis. **(D)** Protein levels of ILK and vascular endothelial growth factor (VEGF) relative to β-actin protein were determined in two groups using semi-quantitative analysis. **(E)** Correlation between ILK levels and EPCs numbers in patients with PE. **(F)** Representative immunoblots for ILK and VEGF in control and PE group. $*p < 0.05$ versus control group.

Dual-staining cells constituted 93% of the total cell population.

Difference between PE group and control group

Representative microscopic images of EPCs from two groups are shown in Figure 2A. As shown in Figure 2B, significantly fewer EPCs were detected in women with PE compared with uncomplicated pregnancy (EPCs number: 52.3 ± 22.1 vs. 97.4 ± 14.1, $p < 0.05$). To further understand the role of ILK in PE, we compared its expression in EPCs from PE group and control group at mRNA and protein levels. Results showed that expressions of *ILK* were detected in EPCs from both groups. Figure 3C illustrates that the expression of ILK was 45% lower in PE patients compared with healthy controls (0.52 ± 0.15 vs. 1.0 ± 0.22, $p < 0.05$). The protein levels of VEGF, an important regulator in angiogenesis, were also decreased in PE (Fig. 3D, F). The correlation of ILK level with average number of EPCs per microscopic field approached significance in the

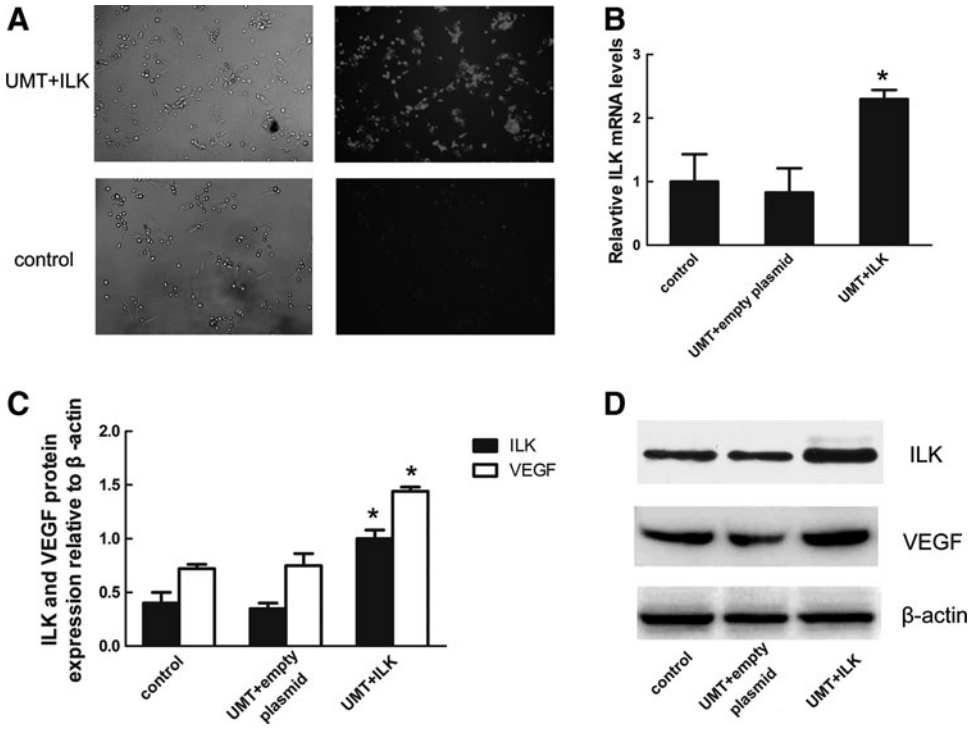

FIG. 3. ILK overexpression in EPCs *in vitro*. **(A)** EPCs in bright field and the same dark field. Most of the early EPC in UMT + ILK group were labeled with red fluorescence. **(B)** mRNA level of ILK in the EPCs of three groups after transfection. **(C)** Densitometric analysis of ILK and VEGF protein relative to β-actin protein in three groups. **(D)** Representative western immunoblotting showing *ILK* and *VEGF* protein expression in control, UMT + empty plasmid, and UMT + ILK groups $*p < 0.05$ versus control and empty plasmid group. UMT, ultrasonic microbubble technique.

Table 2. Cell Viability with Various Ultrasound Intensities and Exposure Time

	Cell viability (%)	
Intensity (W/cm^2)	*30 s*	*60 s*
0	97.4 ± 1.9	97.9 ± 2.3
0.25	96.2 ± 1.6	95.8 ± 1.8
0.5	94.1 ± 2.1	76.3 ± 3.8
0.75	70.2 ± 3.1	53.7 ± 4.4
1	33.5 ± 2.0	21.7 ± 3.9

Values are mean ± SD. The vitality of cells is not affected when the ultrasound is conducted with no more than 0.5 W/cm^2 and 30 s, but it is decreased dramatically when the intensity is greater than 0.5 W/cm^2 ($p < 0.001$).

PE group ($r = 0.56$, $p < 0.05$), but there was no correlation in the control group (Fig. 3E). These results indicated that an insufficiency of ILK may be involved in PE.

Viability of EPCs in different ultrasound parameters

Before gene transfection, a suitable ultrasound intensity and exposure time were determined from the viability of cells. Cell survival was more than 90% when the ultrasound was conducted with 0.25 or 0.5 W/cm^2, 30 s. As the intensity and time increased simultaneously, cell death significantly increased. Our results indicated that ultrasound exposure within a suitable range would not affect cell survival (Table 2).

Transfection efficiency and gene expression

Due to the slight effect on cell viability, we chose these ultrasound parameters (0.5 W/cm^2, 30 s), as the transfection conditions of the ILK gene, for which cell viability was > 90%. pIRES-ILK-Dsred plasmid contains enhanced Dsred code region. Thus, Dsred expression can reflect the transfection efficiency. Cells were incubated for 48 h after transfection, and then, the expression of Dsred was examined using fluorescence microscopy. As presented in Figure 3A, the control group exhibited very low fluorescence. However, ~82% of Dsred-positive cells were obtained in the UMT + ILK group, which was significantly higher than the control group. The result demonstrated the high transfection efficiency of the ultrasound-mediated microbubble technique.

The mRNA and protein expression of *ILK* were effectively promoted in the UMM + ILK group. The RT-PCR results showed that ILK expression was 2.3-fold higher than that of the control group, while ILK expression in the empty plasmid group did not increase compared with the non-plasmid control (Fig. 3B). Similarly, *ILK* and *VEGF* protein expressions were measured by western blotting, as shown in Figure 3C. The protein levels of ILK and VEGF in the UMT + ILK group were also higher than those in the other two groups. Expressions of *VEGF* and *ILK* in the other two groups were not significantly different (Fig. 3D). Therefore, microbubbles were proved to increase protein expression of ultrasound-assisted gene delivery.

Assessment of EPCs proliferation and apoptosis

Using MTT assays, we observed the cell viability in three groups. More absorbance was observed at 560 nm with *ILK*-transfected cells compared with the control in the MTT assay at 12 h after transfection, although there was no significant difference. Twenty-four hours after transfection, a notable difference in cell viability existed among the ILK-transfected group and other two groups, with an increment of more than 67% in the UMT + ILK group compared with

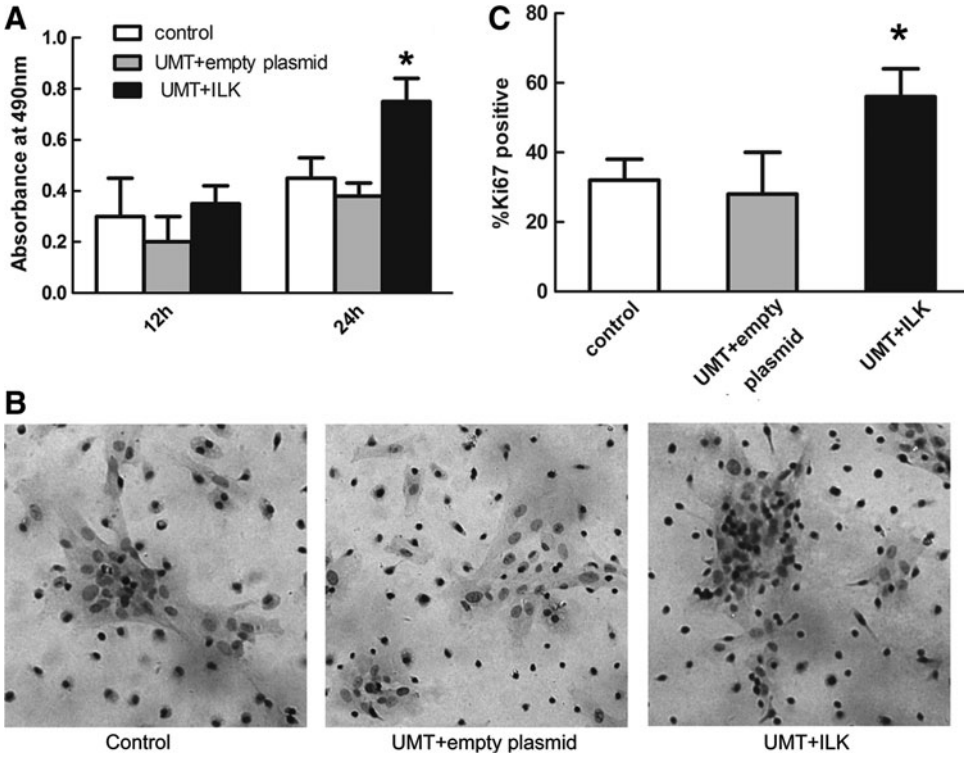

FIG. 4. ILK induced EPCs proliferation. **(A)** Cell viability of EPCs after ILK transfection by MTT assay. **(B)** Ki67 expression of EPCs was detected by immunocytochemistry. Ki67 expression was observed in a few cells in the control and empty plasmid group; in the UMT + ILK group, most of the cells were Ki67 positive. **(C)** The fraction of Ki67-positive cells in the three groups is shown. *$p < 0.05$ versus control and empty plasmid group.

the control group (Fig. 4A). There was no difference in cell viability between the empty plasmid and control group. Next, we performed Ki67 staining (indicative of cells in S/G2 phase) to confirm the cell cycle status as shown in Figure 4B. The fraction of Ki67-positive cells revealed an increasing number of proliferating cells after *ILK* gene transfection (Fig. 4C). To determine whether *ILK* gene repressed cell apoptosis in EPCs, we performed both TUNEL staining and Annexin V-FITC/PI double-staining experiments. In TUNEL assay, the nuclei of the apoptotic cells were stained brown (Fig. 5A). Statistical analysis showed that the percentage of TUNEL-positive cells was decreased after UMT + ILK treatment (8.7%, $p < 0.05$) (Fig. 5C). The following flow cytometry indicated that a considerable decrease in apoptotic cells was observed in the UMT + ILK group compared with the control and empty plasmid group (6.7% vs. 12.4% and 14.3%, $p < 0.05$) at 24 h after transfection (Fig. 5B, D). These data were in accordance with the results of TUNEL staining.

Cell migration and secretion assay

Next, the transwell migration assay was carried out to further explore whether ILK induced migration of EPCs. Since ILK acts as an agitator in migration processes, we investigated the effects of increased ILK on EPCs. The overexpression of ILK significantly promoted the migration of EPCs through the non-matrigel-coated membranes compared with the control group and empty plasmid group, as demonstrated by a remarkable increase in the number of

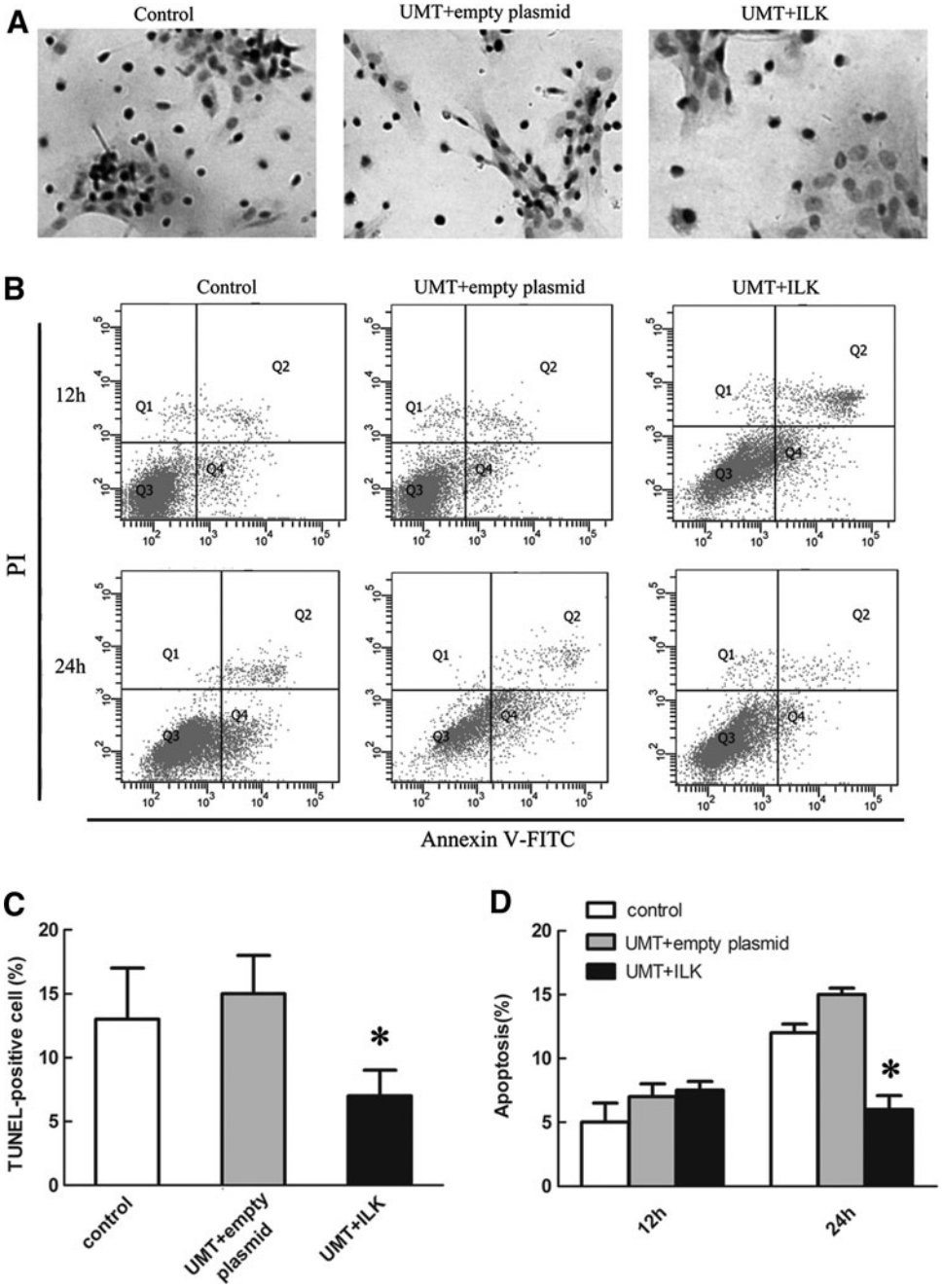

FIG. 5. ILK inhibited EPCs apoptosis. **(A)** UMT + ILK group exhibited a decreased number of TUNEL-positive EPCs. **(B)** Double staining with annexin V-FITC and propidium iodide (PI) demonstrated a decrease in the percentage of apoptotic cells when EPCs were transfected with ILK for 24 h. **(C)** Quantitative analysis of the percentage of brown TUNEL-positive cells. Data shown represent mean ± SD. **(D)** Data of flow cytometry analysis are presented as mean ± SD. *$p < 0.05$ versus control and empty plasmid group.

migrated cells in Figure 6A and B. The amount of VEGF protein secreted from transfected EPCs was evaluated by ELISA *in vitro*. The results showed that there was a significant increase in the amount of VEGF secretion from ILK-transfected EPCs, compared with the untransfected control group and empty plasmid group (Fig. 6C).

Discussion

In this article, we demonstrated that both numbers of EPCs and levels of ILK in EPCs were lower in the PE group than in the normal group. Specific gene delivery to EPCs by ultrasound exposure and microbubbles was achieved using fluorescently labeled pDNA. ILK was amplified notably not only at the mRNA level but also at the protein level after the gene transfection. Furthermore, our findings indicate that the overexpression of *ILK* enhances proliferation, migration, and VEGF secretion, resulting in the angiogenesis of EPCs. Our research has added to understanding the role of ILK and EPCs in PE and provided a safe and feasible way for gene transfection in EPCs. Such EPCs could be developed as therapeutic tools, for either autologous or donor cell therapies in pregnant women with PE.

EPCs constitute a pool of circulating cells that are thought to participate in angiogenesis and ongoing maintenance and repair of the vascular endothelium. Reduced levels of these cells have been shown to be robust predictors of endothelial dysfunction. Consistent with previous studies, we likewise found that EPCs were significantly decreased in PE compared with uncomplicated pregnancy in the first part of our research. The biological mechanisms underlying these observations, however, remain unclear. To further investigate the mechanism, we detected the expression of *ILK* in EPCs. ILK is an important protein that couples growth factors to cascades of downstream signaling events, thereby enhancing their interaction with endothelial cells (Zhang *et al.*, 2002). Using RT-PCR and western blot, we demonstrated that women with PE manifested significantly lower levels of ILK. Moreover, EPCs numbers were positively correlated with ILK levels in the PE group, indicating that ILK level may be the regulatory factor for EPCs number in PE. Through a combination of clinical data and laboratory parameters of PE patients, we hypothesized that deficient ILK may play a major role in the development of endothelial dysfunction in PE.

The findings mentioned earlier suggested that a combinatorial approach using EPCs and ILK may be an effective strategy not only to enhance the functional activity of EPCs but also to provide a novel treatment for PE. However, the transfection of EPCs from pregnant women faces two major problems: efficiency and safety. To date, the viral-based vectors were widely used as the carriers for the genetic modification of EPCs. Many studies have reported the EPCs transfection using lentiviral, retroviral, or adenoviral vectors, and the transfection efficiency could reach as high as 95% (He *et al.*, 2008; Li *et al.*, 2012). Although viral vectors deliver the transgene more efficiently, their high cytotoxicity and immunogenicity may restrict their application. Non-viral vector transfection is safe and easy to apply, but efficiency is an issue affecting the clinical application of stem cell gene therapy. Ultrasonic microbubble gene delivery, a novel non-viral vector transfection, with its high safety and efficiency, can be provided as a feasible tool in gene delivery. Among the physical effects of ultrasound (US), sonoporation is considered the most important and intriguing. Briefly, as the US waves propagate through the medium, the rapid growth in size (rarefaction) and the collapse of microbubbles (compression) lead to the implosion of the microbubbles (Sirsi and Borden, 2012; Zhang *et al.*, 2012). Formation of shock waves, bubble wall motion, and microjets provide the energy for sonoporation of cell membrane. Cell permeability can be transiently altered, enabling free passage of nucleic acids into sonicated cells. By exposure of cells under different ultrasonic intensities (0.25, 0.5, 0.75, and 1.0 W/cm^2) and various time points (30 and 60 s), we demonstrated that ultrasound exposure would not affect cell survival within a suitable range. While outside the

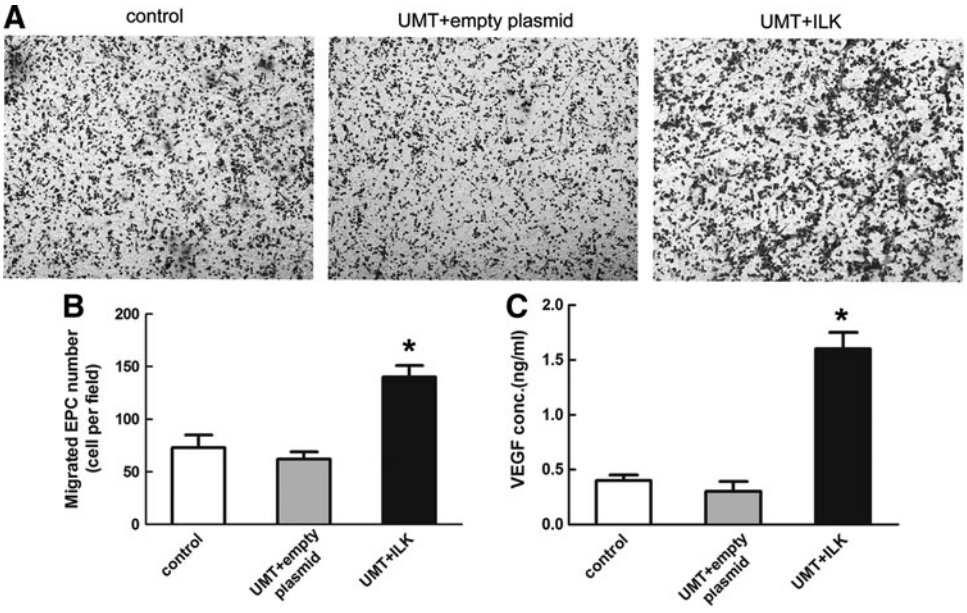

FIG. 6. ILK induced EPCs migration and secretion. **(A)** Representative pictures of migrated cells in three groups. **(B)** The number of migrating cells was increased in the UMT + ILK group than in the other two groups. **(C)** Supernatants from cultured EPCs were collected, and concentrations of VEGF in supernatants were measured by enzyme-linked immunosorbent assay (ELISA) specific kits. *$p < 0.05$ versus control and empty plasmid group.

range, cell death significantly increased as the intensity and time increased simultaneously. Previous studies showed that when the intensity increased gradually, the gene transfection rate increased correspondingly (He *et al.*, 2011). In the current study, we chose 0.5 W/cm^2, 30 s as the optimal ultrasound parameter. Since gene transfection rate was the highest at an intensity of 0.5 W/cm^2, but with subsequent increases in intensity, the cell viability gradually declined. Our results showed that the transfection efficiency of EPCs reached 82%, indicating that ultrasonic microbubble gene delivery could be a useful gene delivery tool.

From the functional experiments of transfected EPCs, we demonstrated that ILK exerts pro-angiogenic functions by promoting cell proliferation, migration, and inhibiting cell apoptosis. Next, we investigated the specific signaling pathways and growth factors by which ILK regulates the EPCs function and angiogenesis. It is well known that VEGF is the most critical growth factor for angiogenesis, and it plays a key role in EC biology. Guo *et al.* (2009) observed that silencing *ILK* with siRNA significantly reduced VEGF secretion in the culture medium of RF/6A cells. So, the observed phenotype in pDNA—ILK EPCs prompted us to investigate the expression of VEGF using western blot and ELISA. The synthetization of VEGF in EPCs was elevated by *ILK* transfection, which was consistent with previous studies. However, we did not explore the specific signal pathways involved in this process. Future work will attempt to examine which signaling pathways are specifically regulated by ILK in the EPCs.

One goal of our research was to elucidate the role of EPCs and ILK in the pathogenesis of PE. Another goal of this study was to find an effective non-viral method to achieve high transfection efficiency in EPCs and to avoid the safety issues caused by the virus transfection. This used method, ultrasound-mediated microbubble in combination with *ILK* transfection, has not been used earlier in EPCs. Although further improvement is required, we think it is still a good and important start toward scientific research and clinical application. Of course, a lot more research is needed to evaluate the safety and feasibility of this method *in vivo*. In summary, our findings shed new light on the pathogenesis of PE and a non-viral method that provides effective modification of EPCs for cell therapy in PE.

Acknowledgment

The project was supported by the National Natural Science Foundation of China; Grant number: (81170584) and (81100442).

Disclosure Statement

No competing financial interests exist.

References

Asahara, T. (1997). Isolation of putative progenitor endothelial cells for angiogenesis. Science **275,** 964–966.

Bekeredjian, R., Kroll, R.D., Fein, E., Tinkov, S., Coester, C., Winter, G., *et al.* (2007). Ultrasound targeted microbubble destruction increases capillary permeability in hepatomas. Ultrasound Med Biol **33,** 1592–1598.

Cavalli, R., Bisazza, A., Trotta, M., Argenziano, M., Civra, A., Donalisio, M., *et al.* (2012). New chitosan nanobubbles for ultrasound-mediated gene delivery: preparation and *in vitro* characterization. Int J Nanomedicine **7,** 3309–3318.

Chen, S., Ding, J.H., Bekeredjian, R., Yang, B.Z., Shohet, R.V., Johnston, S.A., *et al.* (2006). Efficient gene delivery to pancreatic islets with ultrasonic microbubble destruction technology. Proc Natl Acad Sci U S A **103,** 8469–8474.

Chen, W.J., Xiong, Z.A., Tang, Y., Dong, P.T., Li, P., and Wang, Z.G. (2012). Feasibility and effect of ultrasound microbubble-mediated wild-type p53 gene transfection of HeLa cells. Exp Ther Med **3,** 999–1004.

Chesley, L.C. (1980). Hypertension in pregnancy: definitions, familial factor, and remote prognosis. Kidney Int **18,** 234–240.

Cho, H.J., Youn, S.W., Cheon, S.I., Kim, T.Y., Hur, J., Zhang, S.Y., *et al.* (2005). Regulation of endothelial cell and endothelial progenitor cell survival and vasculogenesis by integrin-linked kinase. Arterioscler Thromb Vasc Biol **25,** 1154–1160.

Churdchomjan, W., Kheolamai, P., Manochantr, S., Tapanadechopone, P., Tantrawatpan, C., U-pratya, Y., *et al.* (2010). Comparison of endothelial progenitor cell function in type 2 diabetes with good and poor glycemic control. BMC Endocr Disord **10,** 5.

Gao, D., Xu, Z., Zhang, X., Zhu, C., Wang, Y., and Min, W. (2013). Cadmium triggers kidney cell apoptosis of purse red common carp (*Cyprinus carpio*) without caspase-8 activation. Dev Comp Immunol **41,** 728–737.

Guo, L., Yu, W., Li, X., Zhao, G., and He, P. (2009). Targeting of integrin-linked kinase with a small interfering RNA inhibits endothelial cell migration, proliferation and tube formation *in vitro*. Ophthalmic Res **42,** 213–220.

Han, X., Cheng, W., Jing, H., Zhang, J.W., and Tang, L.L. (2012). Neuroepithelial transforming protein 1 short interfering RNA-mediated gene silencing with microbubble and ultrasound exposure inhibits the proliferation of hepatic carcinoma cells *in vitro*. J Ultrasound Med **31,** 853–861.

Hannigan, G.E., Leung-Hagesteijn, C., Fitz-Gibbon, L., Coppolino, M.G., Radeva, G., Filmus, J., *et al.* (1996). Regulation of cell adhesion and anchorage-dependent growth by a new beta 1-integrin-linked protein kinase. Nature **379,** 91–96.

He, T., Lu, T., d'Uscio, L.V., Lam, C.F., Lee, H.C., and Katusic, Z.S. (2008). Angiogenic function of prostacyclin biosynthesis in human endothelial progenitor cells. Circ Res **103,** 80–88.

He, Y., Bi, Y., Hua, Y., Liu, D., Wen, S., Wang, Q., *et al.* (2011). Ultrasound microbubble-mediated delivery of the siRNAs targeting MDR1 reduces drug resistance of yolk sac carcinoma L2 cells. J Exp Clin Cancer Res **30,** 104.

Hill, J.M., Zalos, G., Halcox, J.P., Schenke, W.H., Waclawiw, M.A., Quyyumi, A.A., *et al.* (2003). Circulating endothelial progenitor cells, vascular function, and cardiovascular risk. N Engl J Med **348,** 593–600.

Hur, J., Yang, H.M., Yoon, C.H., Lee, C.S., Park, K.W., Kim, J.H., *et al.* (2007). Identification of a novel role of T cells in postnatal vasculogenesis: characterization of endothelial progenitor cell colonies. Circulation **116,** 1671–1682.

King, T.F., Bergin, D.A., Kent, E.M., Manning, F., Reeves, E.P., Dicker, P., *et al.* (2013). Endothelial progenitor cells in mothers of low-birthweight infants: a link between defective placental vascularization and increased cardiovascular risk? J Clin Endocrinol Metab **98,** E33–E39.

Li, W., Wang, H., Kuang, C.Y., Zhu, J.K., Yu, Y., Qin, Z.X., *et al.* (2012). An essential role for the Id1/PI3K/Akt/NFkB/

survivin signalling pathway in promoting the proliferation of endothelial progenitor cells *in vitro*. Mol Cell Biochem **363,** 135–145.

Lin, C., Rajakumar, A., Plymire, D.A., Verma, V., Markovic, N., and Hubel, C.A. (2009). Maternal endothelial progenitor colony-forming units with macrophage characteristics are reduced in preeclampsia. Am J Hypertens **22,** 1014–1019.

Malan, D., Elischer, A., Hesse, M., Wickstrom, S.A., Fleischmann, B.K., and Bloch, W. (2013). Deletion of integrin linked kinase in endothelial cells results in defective RTK signaling caused by caveolin 1 mislocalization. Development **140,** 987–995.

Patil, S.D., Rhodes, D.G., and Burgess, D.J. (2005). DNA-based therapeutics and DNA delivery systems: a comprehensive review. AAPS J **7,** E61–E77.

Sirsi, S.R., and Borden, M.A. (2012). Advances in ultrasound mediated gene therapy using microbubble contrast agents. Theranostics **2,** 1208–1222.

Song, S.W., Chang, W., Song, B.W., Song, H., Lim, S., Kim, H.J., *et al.* (2009). Integrin-linked kinase is required in hypoxic mesenchymal stem cells for strengthening cell adhesion to ischemic myocardium. Stem Cells **27,** 1358–1365.

Suzuki, R., Oda, Y., Utoguchi, N., and Maruyama, K. (2011). Progress in the development of ultrasound-mediated gene delivery systems utilizing nano- and microbubbles. J Control Release **149,** 36–41.

Vannucci, L., Lai, M., Chiuppesi, F., Ceccherini-Nelli, L., and Pistello, M. (2013). Viral vectors: a look back and ahead on gene transfer technology. New Microbiol **36,** 1–22.

Wang, F., Wang, Y., Zhang, L., and Zou, L. (2011). Gene modification with integrin-linked kinase improves function of endothelial progenitor cells in pre-eclampsia *in vitro*. J Cell Biochem **112,** 3103–3111.

Wu, C., and Dedhar, S. (2001). Integrin-linked kinase (ILK) and its interactors: a new paradigm for the coupling of extracellular matrix to actin cytoskeleton and signaling complexes. J Cell Biol **155,** 505–510.

Xing, W., Gang, W.Z., Yong, Z., Yi, Z.Y., Shan, X.C., and Tao, R.H. (2008). Treatment of xenografted ovarian carcinoma using paclitaxel-loaded ultrasound microbubbles. Acad Radiol **15,** 1574–1579.

Yan, T., Liu, Y., Cui, K., Hu, B., Wang, F., and Zou, L. (2013). MicroRNA-126 regulates EPCs function: implications for a role of miR-126 in preeclampsia. J Cell Biochem **114,** 2148–2159.

Zhang, Y., Guo, L., Chen, K., and Wu, C. (2002). A critical role of the PINCH-integrin-linked kinase interaction in the regulation of cell shape change and migration. J Biol Chem **277,** 318–326.

Zhang, Y., Tachibana, R., Okamoto, A., Azuma, T., Sasaki, A., Yoshinaka, K., *et al.* (2012). Ultrasound-mediated gene transfection *in vitro*: effect of ultrasonic parameters on efficiency and cell viability. Int J Hyperthermia **28,** 290–299.

Address correspondence to:
Li Zou, MD, PhD
Department of Obstetrics and Gynecology
Union Hospital
Huazhong University of Science and Technology
Wuhan 430022
China

E-mail: medzouli@hotmail.com

Received for publication October 16, 2013; received in revised form January 21, 2014; accepted January 22, 2014.